A&A manuscript no.
(will be inserted by hand later)

Your thesaurus codes are:
05 (10.15.2 (NGC 1960, NGC 2194); 05.01.1; 08.11.1; 08.08.1; 08.12.3)

ASTRONOMY AND ASTROPHYSICS
April 14, 2000

Photometric and kinematic studies of open star clusters. II. NGC 1960 (M 36) and NGC 2194*

Jörg Sanner[1], **Martin Altmann**[1], **Jens Brunzendorf**[2], **Michael Geffert**[1]

[1] Sternwarte der Universität Bonn, Auf dem Hügel 71, D–53121 Bonn, F.R. Germany
[2] Thüringer Landessternwarte Tautenburg, Sternwarte 5, D–07778 Tautenburg, F.R. Germany

Received 7 December 1999, accepted 14 March 2000

Abstract. We present CCD photometry and proper motion studies of the two open star clusters NGC 1960 (M 36) and NGC 2194. Fitting isochrones to the colour magnitude diagrams, for NGC 1960 we found an age of $t = 16$ Myr and a distance of roughly $d = 1300$ pc and for NGC 2194 $t = 550$ Myr and $d = 2900$ pc, respectively. We combined membership determination by proper motions and statistical field star subtraction to derive the initial mass function of the clusters and found slopes of $\Gamma = -1.23 \pm 0.17$ for NGC 1960 and $\Gamma = -1.33 \pm 0.29$ for NGC 2194. Compared to other IMF studies of the intermediate mass range, these values indicate shallow mass functions.

Key words: open clusters and associations: individual: NGC 1960 (M 36), NGC 2194 – astrometry – stars: kinematics – Hertzsprung-Russell and C-M diagrams – stars: luminosity function, mass function

1. Introduction

The shape of the initial mass function (IMF) is an important parameter to understand the fragmentation of molecular clouds and therefore the formation and development of stellar systems. Besides studies of the Solar neighbourhood (Salpeter 1955, Tsujimoto et al. 1997), work on star clusters plays a major role (Scalo 1986) in this field, as age, metallicity, and distance of all stars of a star cluster can generally be assumed to be equal.

Restricted to certain mass intervals, the IMF can be described by a power law in the form

$$\mathrm{d}\log N(m) \sim m^{\Gamma}\,\mathrm{d}\log m. \quad (1)$$

In this notation the "classical" value found by Salpeter (1955) for the Solar neighbourhood is $\Gamma = -1.35$. Average values for Γ from more recent studies, mostly of star clusters, can be found, e.g., in Scalo (1998):

$$\begin{aligned} \Gamma &= -1.3 \pm 0.5 \quad \text{for} \quad m > 10 M_\odot, \\ \Gamma &= -1.7 \pm 0.5 \quad \text{for} \quad 1 M_\odot < m < 10 M_\odot, \text{ and} \\ \Gamma &= -0.2 \pm 0.3 \quad \text{for} \quad m < 1 M_\odot, \end{aligned} \quad (2)$$

where the "±" values refer to a rough range of the slopes derived for the corresponding mass intervals, caused by empirical uncertainties or probable real IMF variations.

Knowledge of membership is essential to derive the IMF especially of open star clusters, where the contamination of the data with field stars presents a major challenge. Two methods for field star subtraction are in use nowadays: separating field and cluster stars by means of membership probabilities from stellar proper motions on one hand, statistical field star subtraction on the other hand. Our work combines these two methods: The proper motions are investigated for the bright stars of the clusters, down to the completeness limit of the photographic plates used, whereas the fainter cluster members are selected with statistical considerations.

From the cleaned data we derive the luminosity and mass functions of the clusters. Including the proper motions, we expect to receive a more reliable IMF, since the small number of bright stars in open clusters would lead to higher uncertainties, if only statistical field star subtraction were applied.

This is the second part of a series of studies of open star clusters, following Sanner et al. (1999). Here we present data on two clusters of the northern hemisphere, NGC 1960 (M 36) and NGC 2194.

NGC 1960 (M 36) is located at $\alpha_{2000} = 5^{\mathrm{h}}36^{\mathrm{m}}6^{\mathrm{s}}$, $\delta_{2000} = +34°8'$ and has a diameter of $d = 10'$ according to the Lyngå (1987) catalogue. Morphologically, NGC 1960 is dominated by a number of bright ($V \lesssim 11$ mag) stars, whereas the total stellar density is only marginally enhanced compared to the surrounding field. The cluster has not yet been studied by means of CCD photometry. Photographic photometry was published by Barkhatova et al. (1985), photoelectric photometry of 50 stars in the region of the cluster by Johnson & Morgan (1953). The most recent proper motion studies are from Meurers (1958) and Chian & Zhu (1966). As their epoch differences between first and second epoch plates (36 and 51 years, respectively) are smaller than ours and today's measuring techniques can be

Send offprint requests to: Jörg Sanner, jsanner@astro.uni-bonn.de

* partly based on data observed at the German-Spanish Astronomical Centre, Calar Alto, operated by the Max-Planck-Institute for Astronomy, Heidelberg, jointly with the Spanish National Commission for Astronomy

Table 1. Typical photometric errors for stars in different magnitude ranges

magnitude range	ΔV [mag]	$\Delta(B-V)$ [mag]
$V <$ 12 mag	0.01	0.01
12 mag $< V <$ 16 mag	0.02	0.04
16 mag $< V$	0.04	0.08

assumed to be more precise we are confident to gain more reliable results.

Tarrab (1982) published an IMF study of 75 open star clusters, among them NGC 1960, and found an exteme value for the slope of (in our notation) $\Gamma = -0.24 \pm 0.05$ for this object. Her work includes only 25 stars in the mass range $3.5M_\odot \lesssim m \lesssim 9M_\odot$, so that a more detailed study covering more members and reaching towards smaller masses is necessary.

For NGC 2194 (located at $\alpha_{2000} = 6^{\rm h}13^{\rm m}48^{\rm s}$, $\delta_{2000} = +12°48'$, diameter $d = 9'$), our work is the first proper motion study according to van Leeuwen (1985). The *RGU* photographic photometry of del Rio (1980) is the most recent publication on NGC 2194 including photometric work.

The cluster is easily detectable as it contains numerous intermediate magnitude (13 mag $\lesssim V \lesssim$ 15 mag) stars, although bright stars with $V \lesssim$ 10 mag are lacking.

In Sect. 2, we present the data used for our studies and the basic steps of data reduction and analysis. Sects. 3 and 4 include the proper motion studies, an analysis of the colour magnitude diagrams (CMDs), and determination of the IMF of the clusters. We conclude with a summary and discussion in Sect. 5.

2. The data and data reduction

2.1. Photometry

CCD images of both clusters were taken with the 1.23 m telescope at Calar Alto Observatory on October 15, 1998, in photometric conditions. The seeing was of the order of 3″. The telescope was equipped with the 1024 × 1024 pix CCD chip TEK 7_12 with a pixel size of 24 μm × 24 μm and the WWFPP focal reducing system (Reif et al. 1995). This leads to a resolution of 1.″0 pix^{-1} and a field of view of 17′ × 17′. Both clusters were observed in Johnson B and V filters, the exposure times were 1 s, 10 s, and 600 s in V, and 2 s, 20 s, and 900 s in B. Figs. 1 and 2 show CCD images of both clusters.

The data were reduced with the DAOPHOT II software (Stetson 1991) running under IRAF. From the resulting files, we deleted all objects showing too high photometric errors as well as sharpness and χ values. The limits were chosen individually for each image, typical values are 0.03 mag to 0.05 mag for the magnitudes, ±0.5 to 1 for sharpness, and 2 to 4 for χ.

Resulting photometric errors of the calibrated magnitudes in different V ranges valid for both clusters as given by the PSF fitting routine are given in Table 1.

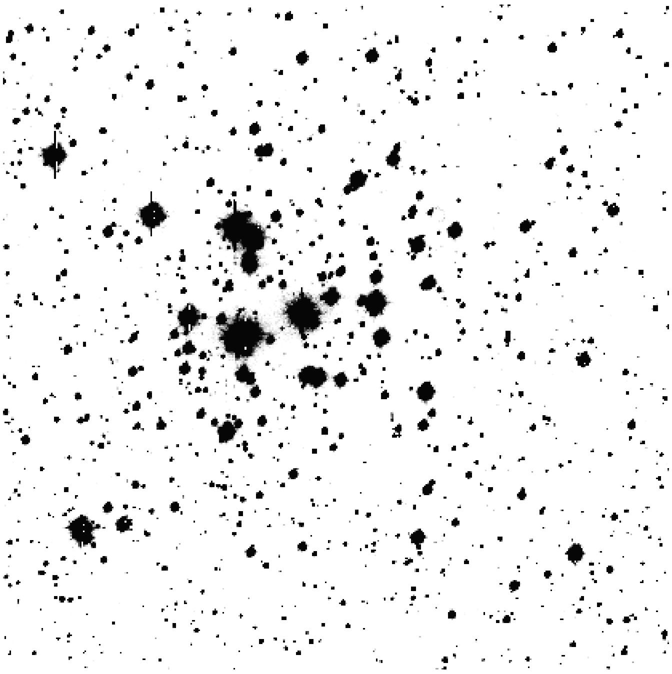

Fig. 1. 600 s V CCD image of NGC 1960. The field of view is approximately 14′ × 14′, north is up, east to the left

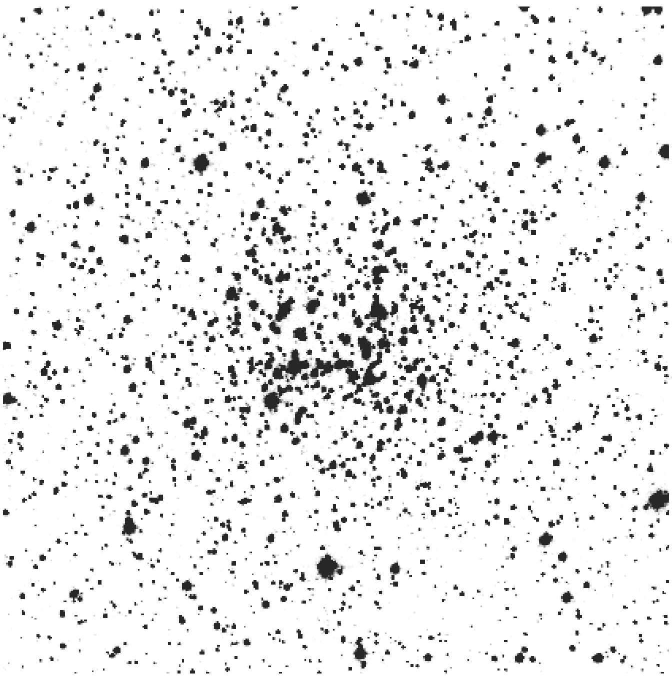

Fig. 2. 600 s V CCD image of NGC 2194. As in Fig. 1, the field of view is approximately 14′ × 14′ with north up and east to the left

The data were calibrated using 44 additional observations of a total of 27 Landolt (1992) standard stars. After correcting the instrumental magnitudes for atmospheric extinction and to exposure times of 1 s, we used the following equations for transformation from instrumental to apparent magnitudes:

$$v - V = z_V - c_V \cdot (B - V) \tag{3}$$

Table 2. List of the photometric data of all stars measured in the CCD field of NGC 1960. For cross-identification, the star numbers of Boden (1951) are given, too. Only the ten brightest stars for which both photometry and proper motions were determined are listed here, the complete table is available online at the CDS archive

No.	Boden No.	x	y	V [mag]	$B-V$ [mag]
1		432.729	550.012	8.83	+0.03
2	23	349.018	441.873	8.91	+0.02
3	138	157.530	819.617	8.95	+0.05
4	101	124.550	353.711	9.05	+0.11
5	61	245.181	427.961	9.07	+0.03
8	27	291.005	555.456	9.52	+0.06
9	48	524.133	537.383	9.52	+0.08
10	21	372.126	456.779	9.72	+0.06
11	38	339.012	698.830	9.88	+0.08
12	184	774.058	850.419	9.94	+1.02
⋮	⋮	⋮	⋮	⋮	⋮

$$(b-v)-(B-V) = z_{B-V} - c_{B-V}\cdot(B-V) \quad (4)$$

where capital letters represent apparent and lower case letters (corrected as described above) instrumental magnitudes. The extinction coefficients k_V and k_{B-V}, zero points z_V and z_{B-V} as well as the colour terms c_V and c_{B-V} were determined with the IRAF routine `fitparams` as:

$$\begin{aligned} k_V &= 0.14 \pm 0.02, \quad k_{B-V} = 0.19 \pm 0.03 \\ z_V &= 2.52 \pm 0.04, \quad z_{B-V} = 0.88 \pm 0.04 \\ c_V &= 0.09 \pm 0.01, \quad c_{B-V} = 0.19 \pm 0.01. \end{aligned} \quad (5)$$

We checked the quality of these parameters by reproducing the apparent magnitudes of the standard stars from the measurements. The standard deviations derived were $\sigma_V = 0.02$ mag and $\sigma_{B-V} = 0.06$ mag.

Johnson & Morgan (1953) published photoelectic photometry of 50 stars in the region of NGC 1960. Their results coincide with ours with a standard deviation of approx. 0.03 mag in V and 0.02 mag in $B-V$, respectively. There is only one exception, star 110 (Boden's (1951) star No. 46) for which we found $V = 14.25$ mag, $B-V = 0.66$ mag, which differs by $\Delta V \approx 2$ mag and $\Delta(B-V) \approx 0.3$ mag from the value of Johnson & Morgan (1953). In their photographic photometry, Barkhatova et al. (1985) found values for this star which coincide with ours. We therefore assume the difference most likely to be caused by a mis-identification of this star by Johnson & Morgan (1953).

All stars for which B and V magnitudes could be determined are listed in Tables 2 (NGC 1960, 864 stars) and 3 (NGC 2194, 2120 stars), respectively. We derived the CMDs of the two clusters which are shown in Figs. 3 and 4. A detailed discussion of the diagrams is given in Sects. 3 and 4.

2.2. Actual cluster sizes

Mass segregation might lead to a larger "true" cluster size than stated, e.g., in the Lyngå (1987) catalogue: While the high mass stars are concentrated within the inner part of the cluster, the lower mass stars might form a corona which can reach as far out as the tidal radius of the cluster (see, e.g., the recent work of Raboud & Mermilliod 1998). Therefore, the range of the cluster stars had to be checked. We applied star counts in concentric rings around the centre of the clusters.

Star counts in the vicinity of NGC 2194 show no significant variations of the stellar density outside a circle with a diameter of $10'$ (corresponding to ≈ 8.5 pc at the distance of the object)

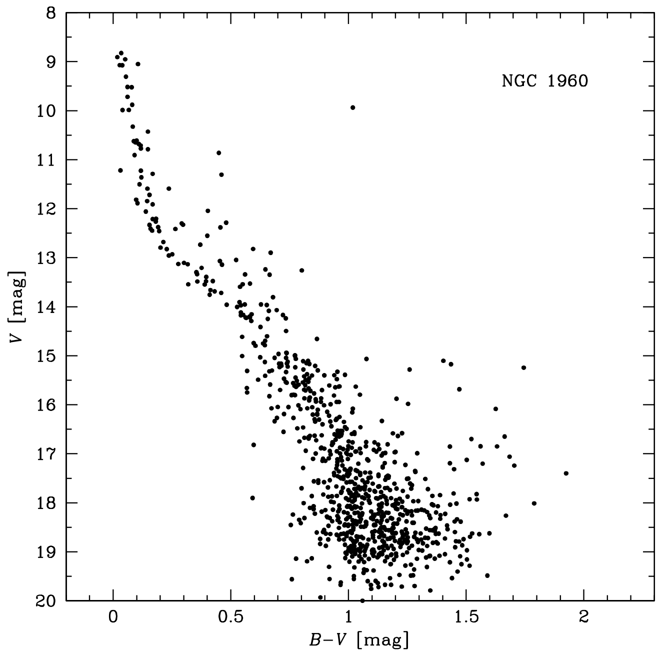

Fig. 3. Colour magnitude diagram of NGC 1960 and the surrounding field. This diagram contains all stars for which both B and V magnitudes were determined. Stars with too high photometric errors were excluded beforehand. This CMD is still contaminated with field stars. For a CMD which is field star corrected see Fig. 10

Table 3. List of the photometric data of all stars measured in the CCD field of NGC 2194. As for Table 2, only the ten brightest stars for which we derived photometric data and proper motions are mentioned here. As a cross reference, the numbers from del Rio (1980) are added. The complete table is available at the CDS archive

No.	del Rio No.	x	y	V [mag]	$B-V$ [mag]
1		591.957	790.526	10.26	+0.66
2		1010.094	706.577	10.47	+0.25
3		434.371	282.158	10.97	+0.71
4	39	522.864	581.859	11.17	+1.77
5		978.803	947.148	11.38	+0.34
6		344.500	740.752	11.48	+1.09
7	49	552.482	537.831	11.50	+1.72
8		634.918	899.808	11.63	+0.12
10	14	646.659	554.135	12.16	+2.40
11		867.565	756.487	12.17	+0.15
⋮	⋮	⋮	⋮	⋮	⋮

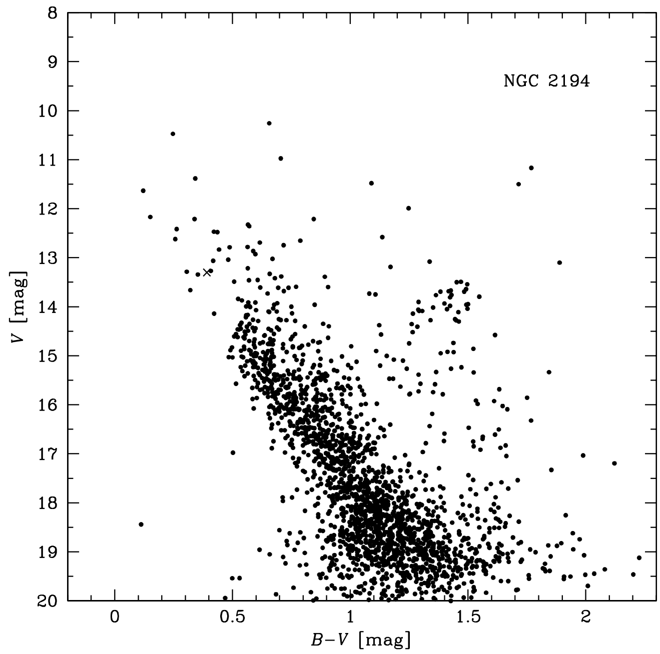

Fig. 4. Colour magnitude diagram of all stars in the field of NGC 2194. For further remarks see Fig. 3. The star marked with a cross is claimed to be a blue straggler by Ahumada & Lapasset (1995). This statement is discussed in Sect. 4.2. Fig. 14 shows the field star corrected CMD of NGC 2194

around the centre of the cluster. For NGC 1960, this point is more difficult to verify, since its total stellar density is much lower than for NGC 2194, so that it is not as easy to see at which point a constant level is reached, and on the other hand, its smaller distance lets us reach fainter absolute magnitudes so that the effect of mass segregation might be more prominent within the reach of our photometry. However, our tests provided evidence, too, that the cluster diameter is no larger than $12'$. It must be stressed that these figures can only provide lower limits for the real cluster sizes: Members fainter than the limiting magnitude of our photometry might reach further out from the centres of the clusters.

2.3. Proper motions

For our proper motion studies we used photographic plates which were taken with the Bonn Doppelrefraktor, a 30 cm refractor ($f = 5.1$ m, scale: $40\farcs44$ mm^{-1}) which was located in Bonn from 1899 to 1965 and at the Hoher List Observatory of Bonn University thereafter. The 16 cm × 16 cm plates cover a region of $1.6° \times 1.6°$. They were completely digitized with 10 μm linear resolution with the Tautenburg Plate Scanner, TPS (Brunzendorf & Meusinger 1998, 1999). The positions of the objects detected on the photographic plates were determined using the software `search` and `profil` provided by the Astronomisches Institut Münster (Tucholke 1992).

In addition, we used the 1 s to 20 s Calar Alto exposures to improve data quality and — for NGC 2194 — to extend the maximum epoch difference. Furthermore, a total of 16 CCD frames of NGC 1960 which were taken with the 1 m Cassegrain telescope ($f/3$ with a focal reducing system) of the Hoher List Observatory were included in the proper motion study. The latter observations cover a circular field of view of $28'$ in diameter which provides a sufficiently large area for the cluster itself and the surrounding field. The astrometric properties of this telescope/CCD camera system were proven to be suitable for this kind of work in Sanner et al. (1998). The stellar (x, y) positions were extracted from the CCD frames with DAOPHOT II routines (Stetson 1991). A list of the plates and Hoher List CCD images included in our study can be found in Table 4.

Table 4. Photographic plates form the Bonn Doppelrefraktor (prefix "R") and CCD frames of the 1m Cassegrain telescope of the Hoher List Observatory (prefix "hl") used to determine the proper motions of the stars in and around NGC 1960 and NGC 2194. For both clusters, the short ($t_{\rm exp} \leq 20$ s) Calar Alto CCD photometric data (see Sect. 2.1 were included in the calculations, too

cluster	plate no.	date	$t_{\rm exp}$[min]
NGC 1960	R0238	30.01.1916	20
	R0288	26.01.1917	90
	R0365	21.01.1919	240
	hl01093	15.01.1996	1
	hl01095	15.01.1996	1
	hl01099	15.01.1996	1
	hl01100	15.01.1996	1
	hl01104	15.01.1996	1
	hl01105	15.01.1996	1
	hl01875	08.03.1996	1
	hl01876	08.03.1996	1
	hl01880	08.03.1996	1
	hl01881	08.03.1996	1
	hl01885	08.03.1996	1
	hl01886	08.03.1996	1
	hl02519	12.03.1996	1
	hl02520	12.03.1996	1
	hl02523	12.03.1996	1
	hl02524	12.03.1996	1
	R1902	15.03.1999	60
	R1903	15.03.1999	60
	R1905	17.03.1999	60
NGC 2194	R0297	14.02.1917	20
	R0333	14.02.1918	130
	R0334	15.02.1918	60
	R0336	16.02.1918	10
	R0337	16.02.1918	60
	R1125	01.11.1972	35
	R1142	14.02.1974	60
	R1144	17.02.1974	60

The fields of the photographic plates contain only a very limited number of HIPPARCOS stars (ESA 1997), as summarized in Table 5. Therefore, we decided to use the ACT catalogue (Urban et al. 1998) as the basis for the transformation of the plate coordinates (x, y) to celestial coordinates (α, δ). For NGC 2194 this decision is evident, for NGC 1960 we preferred the ACT data, too, as the brightest HIPPARCOS stars are over-

Table 5. Number of HIPPARCOS and ACT stars inside the field of view of the Doppelrefraktor plates used for the proper motion studies

cluster	HIPPARCOS	ACT
NGC 1960	8	135
NGC 2194	4	82

exposed on several plates, thus lowering the accuracy of positional measurements: It turned out that only three of the HIPPARCOS stars were measured well enough to properly derive their proper motions from our data. The celestial positions of the stars were computed using an astrometric software package developed by Geffert et al. (1997). We obtained good results using quadratic polynomials in x and y for transforming (x, y) to (α, δ) for the photographic plates and cubic polynomials for the CCD images, respectively.

Initial tests in the fields of both clusters revealed that the proper motions computed for some ten ACT stars disagreed with the ACT catalogue values. We assume that this is caused by the varying accuracy of the Astrographic Catalogue which was used as the first epoch material of the ACT proper motions or by unresolved binary stars (see Wielen et al. 1999). We eliminated these stars from our input catalogue.

The proper motions were computed iteratively from the individual positions: Starting with the ACT stars to provide a calibration for the absolute proper motions and using the resulting data as the input for the following step, we derived a stable solution after four iterations. Stars with less than two first and second epoch positions each or a too high error in the proper motions (> 8 mas yr^{-1} in α or δ) were not taken into further account.

To determine the membership probabilities from the proper motions, we selected $18'$ wide areas around the centres of the clusters. This dimension well exceeds the proposed diameter of both clusters so that we can assume to cover all member stars for which proper motions were determined. Furthermore, this region covers the entire field of view of the photometric data. The membership probabilities were computed on the base of the proper motions using the method of Sanders (1971): We fitted a sharp (for the members) and a wider spread (for the field stars) Gaussian distribution to the distribution of the stars in the vector point plot diagram and computed the parameters of the two distributions with a maximum likelihood method. From the values of the distribution at the location of the stars in the diagram we derived the membership probabilities. The *positions* of the stars did not play any role in the derivation of the membership probabilities. In the following, we assumed stars to be cluster members in case their membership probability is 0.8 or higher.

2.4. *Colour magnitude diagrams*

Before analysing the CMDs in detail, we had to distinguish between field and cluster stars to eliminate CMD features which may result from the field star population(s). For the stars down to $V = 14$ mag (NGC 1960) and $V = 15$ mag (NGC 2194) we found after cross-identifying the stars in the photometric and astrometric measurements that our proper motion study is virtually complete. Therefore we used these magnitudes as the limits of our membership determination by proper motions. For the fainter stars we statistically subtracted the field stars:

We assumed a circular region with a diameter of 806 pixels or $13\rlap{.}'4$ to contain all cluster member stars. As seen in Sect. 2.2, this exceeds the diameters of the clusters. The additional advantage of this diameter of the "cluster" region is that this circle corresponds to exactly half of the area covered by the CCD images so that it was not necessary to put different weights on the star counts in the inner and outer regions. We compared the CMDs of the circular regions containing the clusters with the diagrams derived from the rest of the images to determine cluster CMDs without field stars. The method is described in more detail in, e.g., Dieball & Grebel (1998).

We fitted isochrones based on the models of Bono et al. (1997) and provided by Cassisi (private communication) to the cleaned CMDs. We assumed a Solar metallicity of $Z = 0.02$ and varied the distance modulus, reddening, and ages of the isochrones. Comparison with the isochrones of other groups (Schaller et al. 1992, Bertelli et al. 1994) does not show any significant differences in the resulting parameters.

2.5. *Mass function*

For the IMF study it is important to correct the data for the incompleteness of our photometry. With artificial star experiments using the DAOPHOT II routine `addstar` we computed B-magnitude depending completeness factors for both clusters. The B photometry was favoured for these experiments since its completeness decreases earlier as a consequence of its brighter limiting magnitude. According to Sagar & Richtler (1991), the final completeness of the photometry after combining the B and V data is well represented by the least complete wavelength band, hence V completeness was not studied. The results, which are approximately the same for both NGC 1960 and NGC 2194, are plotted in Fig. 5: The sample is — except for a few stars which likely are missing due to crowding effects — complete down to $B = 19$ mag, and for stars with $B \lesssim 20$ mag, we still found more than 60 % of the objects. In general, we found that the completeness in the cluster regions does not differ from the values in the outer parts of the CCD field. We therefore conclude that crowding is not a problem for our star counts, even at the faint magnitudes. However, crowding may lead to an increase in the photometric errors, especially in the region of NGC 2194, in which the stellar density is considerably higher than for NGC 1960.

Several objects remained far red- or bluewards of the lower part of the main sequence after statistical field star subtraction. We assume that this results from the imperfect statistics of the sample. For a formal elimination of these stars we had to define a region of the CMD outside of which all objects can be considered to be non-members. This was achieved by shifting the fitted isochrones by two times the errors listed in Table 1 in V and $B - V$ to the lower left and the upper right in the CMD

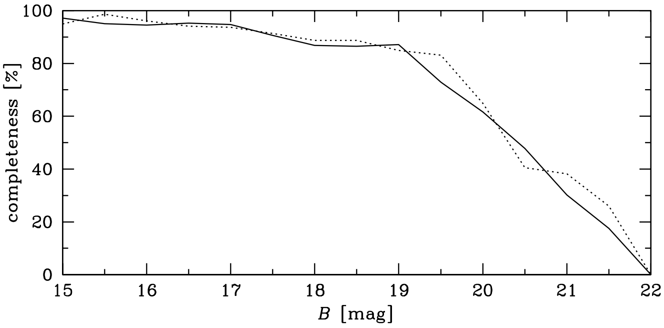

Fig. 5. Completeness of the 900 s B exposures of NGC 1960 (solid line) and NGC 2194 (dotted line). Down to $B = 20$ mag both samples are at least 60 % complete. Note that the IMF is computed on the base of the V magnitudes which alters the completeness function as we deal with main sequence stars with a colour of up to $B - V = 1.5$ mag

(Since this procedure applies only to stars within the range of the statistical field star subtraction, we used the errors given for the faint stars in our photometry.). To take into account probable double or multiple stars we added another 0.75 mag to the shift to the upper right, and for NGC 2194 we allowed another $\Delta(B - V) = 0.2$ mag in the same direction as a consequence of the probably higher photometric errors due to crowding in the central part of the cluster. All stars outside the corridor defined in this way are not taken into account for our further considerations. The shifted isochrones are plotted as dotted lines in Figs. 10 and 14, respectively. It may be remarked that according to Iben (1965) we can exclude objects with a distance of several magnitudes in V or a few tenths of magnitudes in $B - V$ from the isochrone to be pre-main sequence members of neither NGC 1960 nor NGC 2194.

We furthermore selected all objects below the turn-off point of the isochrones. For the remaining stars, we calculated their initial masses on the base of their V magnitudes. We used the mass-luminosity relation provided with the isochrone data. V was preferred for this purpose as the photometric errors are smaller in V compared to the corresponding B magnitudes. The mass-luminosity relation was approximated using $6^{\rm th}$ order polynomials

$$m[M_\odot] = \sum_{i=0}^{6} a_i \cdot (V[\mathrm{mag}])^i \qquad (6)$$

which resulted in an rms error of less than 0.01. Using $5^{\rm th}$ or lower order polynomials caused higher deviations especially in the low mass range. The values of the parameters a_i are listed in Table 6.

Taking into account the incompleteness of the data, we determined the luminosity and initial mass functions of the two clusters. The IMF slope was computed with a maximum likelihood technique. We preferred this method instead of the "traditional" way of a least square fit of the mass function to a histogram, because those histogram fits are not invariant to size and location of the bins: Experiments with shifting the location and size of the bins resulted in differences of the exponent

Table 6. Parameters of the polynomial approximation of the mass-luminosity relation for the stars of the two clusters. See Eq. (6) for the definition of $(a_0, \ldots, a_6)$

	NGC 1960	NGC 2194
a_0	$-3.0892 \cdot 10^{+2}$	$+1.2671 \cdot 10^{+2}$
a_1	$+1.4661 \cdot 10^{+2}$	$-3.5052 \cdot 10^{+1}$
a_2	$-2.6277 \cdot 10^{+1}$	$+4.3076 \cdot 10^{0}$
a_3	$+2.3780 \cdot 10^{0}$	$-2.9135 \cdot 10^{-1}$
a_4	$-1.1671 \cdot 10^{-1}$	$+1.1218 \cdot 10^{-2}$
a_5	$+2.9728 \cdot 10^{-3}$	$-2.3033 \cdot 10^{-4}$
a_6	$-3.0881 \cdot 10^{-5}$	$+1.9556 \cdot 10^{-6}$

of more than $\Delta\Gamma = 0.2$. Fig. 6 shows the results of such an experiment with the NGC 1960 data. The fitted IMFs show an average Γ value of around -1.2 with individual slopes ranging from -1.1 down to -1.4. This can be explained by the very small number of stars in the higher mass bins which contain only between one and ten stars. In case only one member is mis-interpreted as a non-member or vice versa, the corresponding bin height might be affected by up to $\Delta \log N(m) = 0.3$ in the worst case which will heavily alter the corresponding IMF slope. In addition, all *bins* of the histogram obtain the same weight in the standard least square fit, no matter how many stars are included. For very populous or older objects (globular or older open star clusters, see, e.g., the IMF of NGC 2194) this effect plays a minor role, because in these cases the number of stars per bin is much higher. On the other hand, the maximum likelihood method does not lose information (as is done by binning), and each *star* obtains the same weight in the IMF computation.

Nevertheless, for reasons of illustration we sketch the IMF of our two clusters with an underlying histogram in Figs. 12 and 16.

3. NGC 1960

3.1. Proper motion study

With the method described above, we determined the proper motions of 1,190 stars within the entire field of the photographic plates. We found that the limiting magnitude of the second epoch plates is brighter than that of the first epoch plates. This effect is compensated by the addition of the CCD data, so that in the cluster region we reach fainter stars than in the outer region of the field. Therefore, the limiting magnitude of the proper motion study is fainter in the area for which the CCD data were available.

After four iterations of proper motion determination, the comparison of the computed proper motions with ACT led to systematic positional differences of the order of $\Delta\alpha = 0\rlap{.}''04$ and $\Delta\delta = 0\rlap{.}''10$ and for the proper motions of around 0.4 mas yr^{-1}. The internal dispersion of the proper motions was computed from the deviations of the positions from a linear fit of α and δ as functions of time. We derived mean values of $\sigma_{\mu_\alpha \cos\delta} = 1.1$ mas yr^{-1} and $\sigma_{\mu_\delta} = 0.9$ mas yr^{-1} for individual stars.

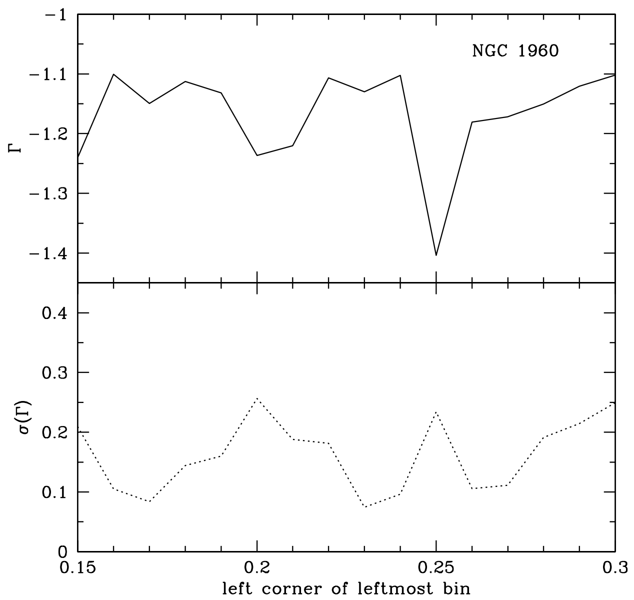

Fig. 6. Results of an experiment with part of the NGC 1960 data. We computed histograms with an equal bin width of $\Delta \log m[M_\odot] = 0.1$ (as in Fig. 12), but varying location of the bins, expressed by the log m value of the left corner of the leftmost bin. This diagram shows the resulting IMF slope Γ and the corresponding error of the fit

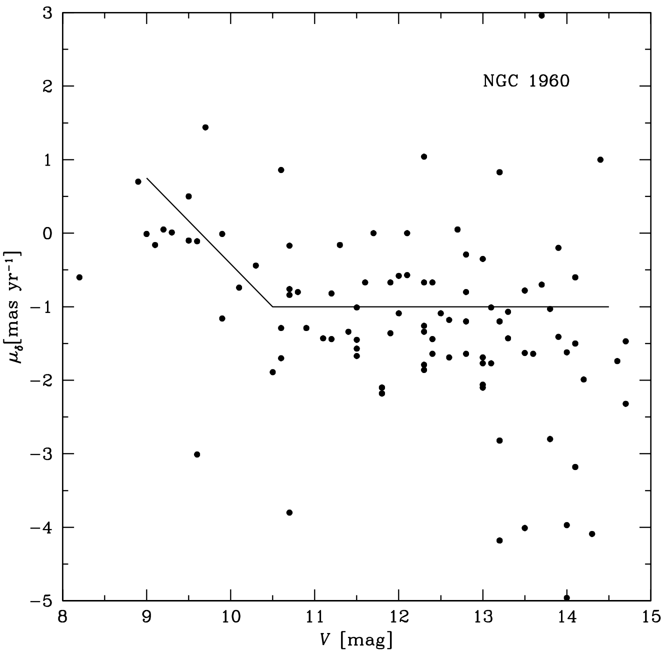

Fig. 7. Dependence of the proper motions in δ on the magnitude for the stars in the field of NGC 1960. The diagram shows a clear magnitude term for the stars brighter than 10.5 mag. Note that these proper motions were computed on the basis of GSC 1.2 so that we deal with *relative* proper motions here. The solid line sketches the mean proper motion for the cluster member stars. See the text for further discussion

We detected a slight, but systematic slope of the proper motions in δ depending on the magnitude of the stars resulting in a difference of approximately 2 mas yr^{-1} for the proper motions between the brightest and faintest members. As the magnitude range of the ACT catalogue within our field of view is limited to approximately 11 mag, we used the positions provided by the Guide Star Catalog (GSC) Version 1.2 (Röser et al. 1998), which covers stars over the entire range of our proper motion study, for further analysis. The disadvantage of GSC is the fact that it does not provide proper motions. Therefore, all results obtained with this catalogue are *relative* proper motions only. Fig. 7 shows the proper motions in δ and their dependence on the magnitudes derived from this computation for the stars in the inner region of the photographic plates. The diagram shows that only the stars brighter than 10.5 mag are influenced by a clear magnitude term leading to deviations of up to 2 mas yr^{-1} with respect to the stars fainter than 10.5 mag which do not show any systematic trend. We included a magnitude term into our transformation model, however, since the behaviour is not linear with magnitudes and different from plate to plate we were unable to completely eliminate the effect. Furthermore, taking into account that many of the ACT stars are brighter than 10.5 mag, it is clear that this deviation was extrapolated over the entire range of the proper motion study.

Meurers (1958), who had used the same first epoch material for his proper motion study, found a similar phenomenon and suggested that the bright and the faint stars in the region of NGC 1960 form independent stellar "aggregates". In his study the proper motion difference between bright and faint stars is much more prominent. Taking into account his smaller epoch difference of 36 years this could be explained assuming that the effect is caused by (at least some of) the first epoch plates on which the positions of the brighter stars seem to be displaced by an amount of approximately $0\farcs1$ to $0\farcs2$ compared to the fainter objects, whereas both his and our second epoch data are unaffected. This proposition would also explain why we did not detect this inaccuracy during the determination of the positions on the plates, since the uncertainties of single positional measurements are of the same order of magnitude.

The proper motions in α proved to be unaffected by this phenomenon.

We found that when using the ACT based proper motions, the membership determination is not affected by this problem, since the magnitude trend in μ_δ is smoothed over the magnitude range (in comparison with Fig. 7). On the other hand, in the GSC solution, the bright stars have proper motions differing too much from the average so that almost all of them are declared non-members. Therefore we used the results based on the ACT data for the computation of the membership probabilities. Table 7 shows a list of all proper motions determined on the base of the ACT catalogue.

The vector point plot diagram as determined on the base of ACT for the stars in the central region of the plates is presented in Fig. 8. Membership determination resulted in 178 members and 226 non-members of NGC 1960. The distribution of mem-

Table 7. List of all stellar proper motions determined from the photographic plates and the additional CCD images of NGC 1960. The positions are given for the epoch 1950.0 in the equinox J2000.0 coordinate stystem. The stellar id numbers are the same as in Table 2. Again, the stellar numbers from Boden (1951) are listed in addition. Only the proper motions of the same stars as in Table 2 are presented here, the complete table is available online at the CDS archive in Strasbourg

No.	Boden No.	α_{2000} [hhmmss.sss]	δ_{2000} [$^\circ$ $'$ $''$]	$\mu_\alpha \cos\delta$ [mas yr^{-1}]	μ_δ
1		053615.805	+340836.81	+2.29	−7.78
2	23	053623.059	+341032.84	+2.28	−8.46
3	138	053639.262	+340349.88	+2.33	−9.55
4	101	053642.305	+341206.09	+3.83	−8.43
5	61	053632.004	+341047.44	+2.36	−8.59
8	27	053628.031	+340830.78	+3.36	−8.02
9	48	053607.902	+340850.53	+1.16	−8.36
10	21	053621.062	+341016.91	+2.46	−8.35
11	38	053623.844	+340557.38	+2.45	−8.61
12	184	053546.469	+340317.47	−5.30	−6.61
⋮	⋮	⋮	⋮	⋮	⋮

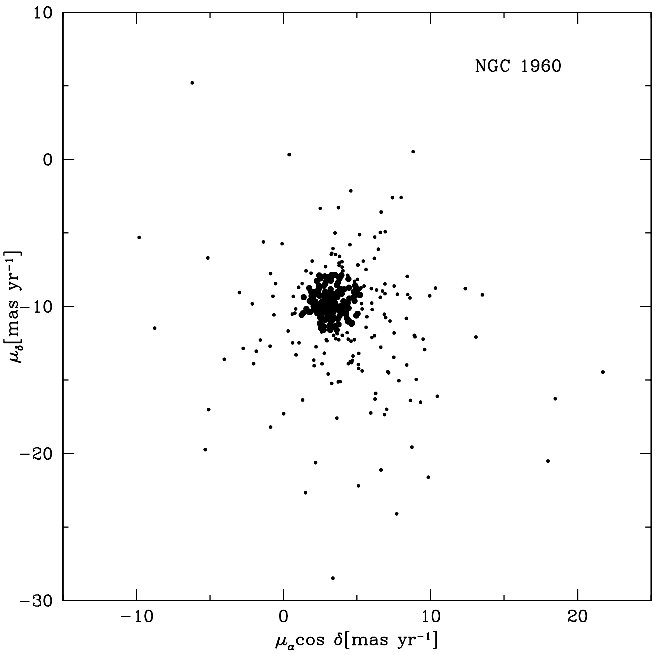

Fig. 8. Vector point plot diagram of the stars in the region of NGC 1960. The stars with a membership probability of less than 0.8 are indicated by small, the others by larger dots. The width of the distribution of the stars with a high membership probability is of the order of 1 mas yr^{-1} which coincides with the standard deviation of the proper motion of a single star

bership probabilities sketched in Fig. 9 shows a clear separation of members and non-members with only a small number of stars with intermediate membership probabilities. The centre of the proper motion distribution of the cluster members in the vector point plot diagram is determined to be

$$\mu_\alpha \cos\delta \;=\; 3.2 \pm 1.1 \text{ mas yr}^{-1} \text{ and} \tag{7}$$
$$\mu_\delta \;=\; -9.8 \pm 0.9 \text{ mas yr}^{-1}. \tag{8}$$

The width of the Gaussian distribution of the proper motions is around 1 mas yr^{-1} and hence the same as the 1σ error of the proper motion of a single object. The field moves very similarly with

$$\mu_\alpha \cos\delta \;=\; 4.4 \pm 5 \text{ mas yr}^{-1} \text{ and} \tag{9}$$
$$\mu_\delta \;=\; -11.4 \pm 5 \text{ mas yr}^{-1}. \tag{10}$$

The similarity of field and cluster proper motions makes membership determination a difficult task: Several field stars which by chance have the same proper motion as the cluster stars will be taken for members.

These results cannot be used for a determination of the *absolute* proper motion of the cluster, since the centre of the distribution can be assumed to be displaced upwards in the vector point plot diagram as a consequence of the magnitude dependence of the μ_δ values. To obtain reliable absolute proper motions, nevertheless, we used the fainter ($>$ 10.5 mag) part of the proper motions computed on the base of GSC 1.2 which are stable with magnitudes and compared their relative proper motions with the values given for the corresponding stars in the ACT. We found a difference of $\Delta(\mu_\alpha \cos\delta) = 1.4 \pm 2.6$ mas yr^{-1} and $\Delta\mu_\delta = -6.5 \pm 2.4$ mas yr^{-1} and centres of the GSC based proper motion distributions of $\mu_\alpha \cos\delta = 1.5 \pm 0.7$ mas yr^{-1} and $\mu_\delta = -1.5 \pm 0.7$ mas yr^{-1}. As a

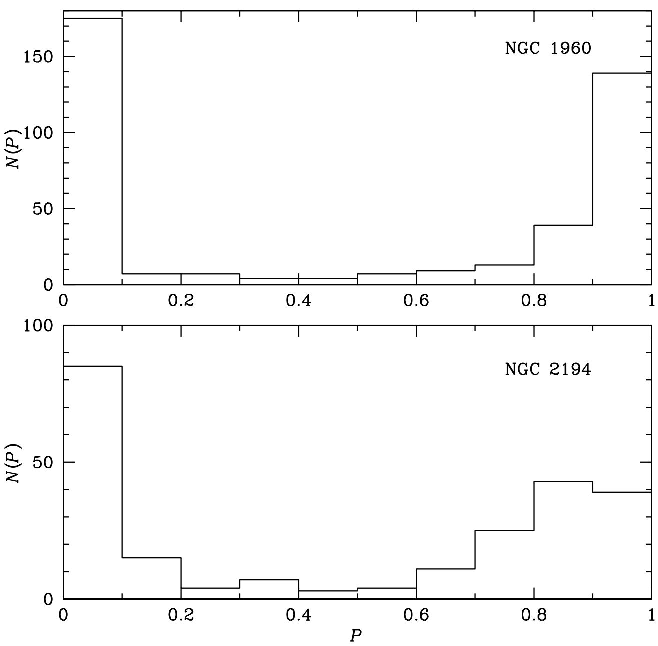

Fig. 9. Histograms of the membership probabilities for the stars of NGC 1960 (upper diagram) and NGC 2194 (lower diagram). All stars with membership probabilities of 0.8 or higher are considered cluster members. Note that the separation between members and non-members is less prominent for NGC 2194 than for NGC 1960

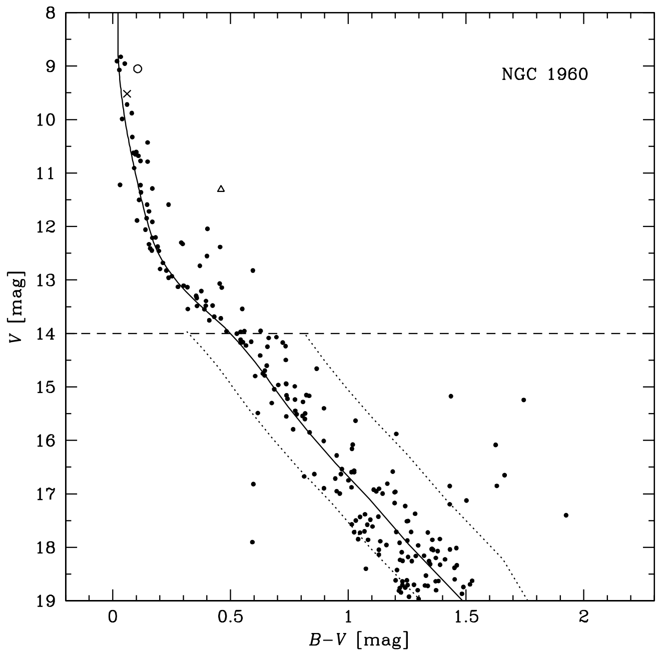

Fig. 10. Colour magnitude diagram of all members of NGC 1960 as determined with the proper motions ($V < 14$ mag) and statistical field star subtraction ($V > 14$ mag). The dashed line stands for the borderline between the two methods of membership determination; the dotted lines indicate the corridor containing the main sequence for the IMF computation (see Sect. 2.5 for details). The parameters of the isochrone plotted in the diagram are listed in Table 8. The three stars marked with special symbols are discussed in Sect. 3.2

consequence we determined the absolute proper motions of NGC 1960 to be

$$\mu_\alpha \cos\delta \;=\; 2.9 \pm 2.7 \text{ mas yr}^{-1} \text{ and} \tag{11}$$

$$\mu_\delta \;=\; -8.0 \pm 2.5 \text{ mas yr}^{-1}. \tag{12}$$

As expected, the value of the proper motion in right ascension is — compared to Eq. (7) — unaffected within the errors, whereas μ_δ is different from the value of Eq. (8) by a value which corresponds to the 2σ error of μ_δ.

3.2. Colour magnitude diagram properties

The CMD of NGC 1960 (Fig. 10) shows a clear and narrow main sequence with an indication of a second main sequence including approximately 15 stars from $V = 11.5$ mag to $V = 14$ mag (corresponding to masses from $m \approx 3.5 M_\odot$ to $m \approx 1.4 M_\odot$). These stars might be Be stars (see, e.g., Zorec & Briot 1991) or unresolved binaries (see, e.g., Abt 1979 or the discussion in Sagar & Richtler 1991).

Slettebak (1985) reports on two Be stars in NGC 1960. One of them, our star 1374 (Boden's (1951) star No. 505, erroneously named No. 504 by Slettebak), clearly fails to fulfil our membership criterion with a proper motion of $\mu_\alpha \cos\delta = -0.7$ mas yr^{-1} and $\mu_\delta = -0.3$ mas yr^{-1}. In addition, it is located so far off the centre of the cluster that it is even outside the field of our CCD images. On the other hand, star 4 (Boden's (1951) star No. 101, $V = 9.05$ mag, $B - V = 0.11$ mag) shows a proper motion of $\mu_\alpha \cos\delta = 3.9$ mas yr^{-1} and $\mu_\delta = -8.8$ mas yr^{-1} which makes it a very likely cluster member with a membership probability of 0.95. In Fig. 10, this object is marked with a circle. A third Be star in the region is mentioned in the WEBDA database (Mermilliod 1999): Boden's (1951) star No. 27, or our star 8. We obtained a proper motion of $\mu_\alpha \cos\delta = 3.36$ mas yr^{-1}, $\mu_\delta = -8.02$ mas yr^{-1}. From these figures we computed a membership probability of 0.89 so that this star is a likely cluster member. We marked this object in Fig. 10 with a cross. As there is no evidence for any further Be stars, it is plausible to assume that the other stars forming the second main sequence most likely are unresolved binary stars.

Table 8. Parameters of NGC 1960 and NGC 2194 as derived from isochrone fitting to the colour magnitude diagram

	NGC 1960
distance modulus	$(m - M)_0 = 10.6 \pm 0.2$ mag
i.e. distance	$r = 1318 \pm 120$ pc
reddening	$E_{B-V} = 0.25 \pm 0.02$ mag
age	$t = 16^{+10}_{-5}$ Myr
i.e.	$\log t = 7.2 \pm 0.2$
metallicity	$Z = 0.02$
	NGC 2194
distance modulus	$(m - M)_0 = 12.3 \pm 0.2$ mag
i.e. distance	$r = 2884 \pm 270$ pc
reddening	$E_{B-V} = 0.45 \pm 0.02$ mag
age	$t = 550 \pm 50$ Myr
i.e.	$\log t = 8.74 \pm 0.05$
metallicity	$Z = 0.02$

The star at $V = 11.3$ mag, $B - V = 0.46$ mag (star 29 of our sample, marked with a triangle in Fig. 10) does not fit to any isochrone which properly represents the other stars in this magnitude range. It shows a proper motion of $\mu_\alpha \cos\delta = 2.9$ mas yr^{-1} and $\mu_\delta = -9.7$ mas yr^{-1} resulting in a membership probability of 0.97. This object may be an example for a star which coincidentally shows the same proper motion as the cluster, but being in fact a non-member.

From our isochrone fit, we derived the parameters given in Table 8. Age determination was quite a difficult task for NGC 1960, as there are no significantly evolved (red) stars present in the CMD. We found that the 16 Myr isochrone might be the optimal one, since it represents the brightest stars better than the (in terms of ages) neighbouring isochrones. The comparably large error we adopted reflects this consideration.

3.3. Initial mass function

The determination of the IMF slope from the completeness corrected data obtained from the CMD (Fig. 10) leads to the value of $\Gamma = -1.23 \pm 0.17$ for NGC 1960 in a mass interval from $m = 9.4 M_\odot$ down to $m = 0.725 M_\odot$ (corresponding to $V = 8.9$ mag to $V = 19$ mag). This restriction was chosen to

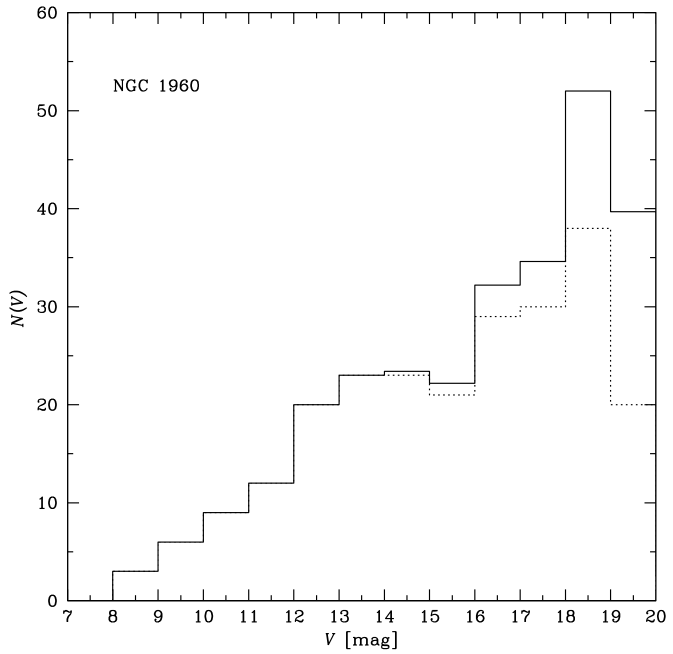

Fig. 11. Luminosity function of NGC 1960. The solid line stands for the completeness corrected data, the dotted line for the uncorrected values. The rightmost bin almost reaches the limit of our photometric study so that it cannot be taken for reliable

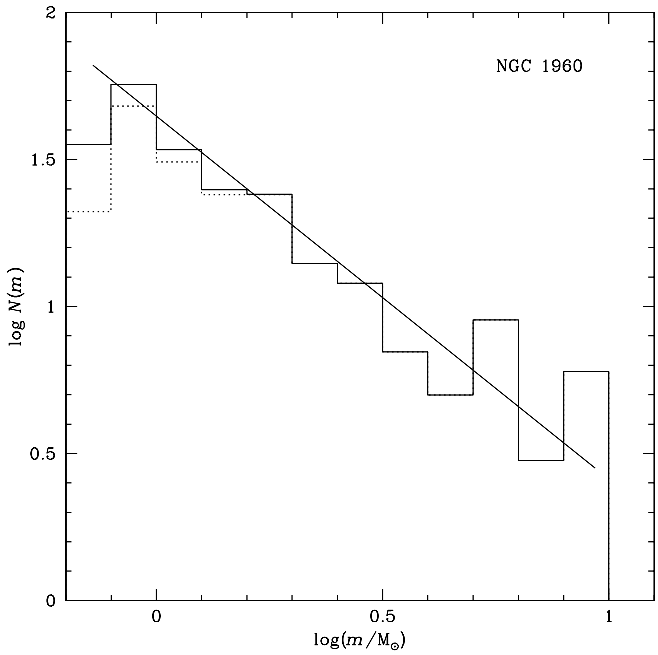

Fig. 12. Initial mass function of NGC 1960. The solid histogram corresponds to the completeness corrected values, the dotted one to the original data. The IMF slope calculated with a maximum likelihood analysis is determined to be $\Gamma = -1.23 \pm 0.17$. The stars with $m < 0.725 M_\odot$ (i.e. $\log(m/M_\odot) < -0.14$) were not taken into account for the slope determination as the average completeness for those stars is below 60 %. The limits of the IMF line illustrate the mass range under consideration. The probable binary nature of some objects is not taken into account in this plot

guarantee a completeness of the photometry of at least 60 %. To test the stability of the IMF concerning the probable double star nature of several objects, we assumed the stars above the brighter part of the main sequence (a total of 18 objects) to be unresolved binary stars with a mass ratio of 1 and computed the IMF of this modified sample, as well. The slope increased to the value of $\Gamma = -1.19 \pm 0.17$ within the same mass range, representing a slightly shallower IMF. Anyway, the influence of a binary main sequence is negligible within the errors. We also experimented with leaving out the magnitude range critical for membership determination (see Sect. 3.1 and Fig. 7), i.e. the stars brighter than $V = 10.5$ mag ($m > 5.75 M_\odot$), and derived $\Gamma = -1.26 \pm 0.2$ — a result which coincides well within the errors with the above ones. This shows once more that the membership determination — and therefore the IMF — was almost not affected by the magnitude term of our proper motion study. Fig. 12 sketches the IMF of NGC 1960.

4. NGC 2194

4.1. Proper motion study

For stars brighter than $V = 9$ mag, some of the plates of NGC 2194 showed a systematic shift of the computed δ positions with respect to the ACT values. We therefore excluded all those stars from our input catalogue. However, this effect — which is different from the one described before for NGC 1960, since it perceptibly affects the positions — does not influence our membership determination as the region of NGC 2194 does not cover any stars of this brightness (see also Table 3).

Proper motions of 2,233 stars could be computed from the plates of NGC 2194. This figure is significantly higher than for NGC 1960, since this time the second epoch plates are of much higher quality, so that we reach fainter stars over the entire $1.6° \times 1.6°$ field. After four iterations of our proper motion determination, the systematic difference between ACT and our results were $0\farcs07$ for the positions and 0.07 mas yr^{-1} for the proper motions. The standard deviation of the proper motions were $\sigma_{\mu_\alpha \cos\delta} = 1.6$ mas yr^{-1} and $\sigma_{\mu_\delta} = 1.5$ mas yr^{-1}. The vector point plot diagram (Fig. 13) of the stars in the region of NGC 2194 shows that the stars are not as highly concentrated in the centre of the distribution of the cluster stars as for NGC 1960. This also explains the less distinct peak for high membership probabilities in the histogram shown in Fig. 9.

Although one finds more stars on the whole plates, in the inner region the proper motions of fewer objects were detected. This is caused by the lower number of sufficiently bright stars in and around the cluster (see Figs. 2 and 4). On the other hand, the low part of the main sequence is much more densely populated. We will see in Sect. 4.2 that the total number of members detected is higher for NGC 2194 than for NGC 1960.

We classified 149 members and 81 non-members. For this cluster, the separation between members and non-members was even more difficult as can be seen from the membership proba-

Table 9. List of all stellar proper motions determined from the photographic plates of NGC 2194. Besides our internal numbering system, the numbers of del Rio's (1980) study are given. For more information see Table 7. The complete table is available online at the CDS archive in Strasbourg

No.	del Rio No.	α_{2000} [hhmmss.sss]	δ_{2000} [° ′ ″]	$\mu_\alpha \cos\delta$ [mas yr^{-1}]	μ_δ [mas yr^{-1}]
1		061346.145	+124352.43	−88.08	+19.39
2		061315.582	+124525.58	+2.46	−1.61
3		061357.445	+125258.92	+9.64	−14.54
4	39	061350.910	+124736.25	−0.43	+1.65
5		061318.016	+124113.11	−4.77	−1.43
6		061403.945	+124446.31	−1.88	−2.28
7	49	061348.746	+124823.41	−4.13	+5.11
8		061342.734	+124158.29	−0.16	−2.58
10	14	061341.836	+124806.10	−4.12	+4.38
11		061325.805	+124431.25	+0.92	−0.08
⋮	⋮	⋮	⋮	⋮	⋮

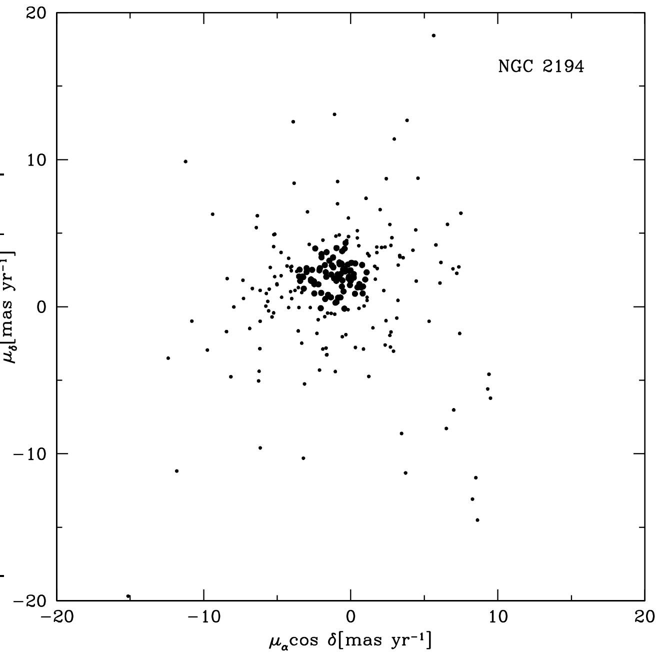

Fig. 13. Vector point plot diagram of the stars in the region of NGC 2194. As in Fig. 8, the stars with a membership probability of higher than 0.8 are indicated by large, the others by small dots. The single errors are of the order of 1.5 mas yr^{-1}

bility histogram plotted in Fig. 9: Approximately 50 stars show intermediate membership probabilities between 0.2 and 0.8. The result for the absolute proper motion of the cluster is

$$\mu_\alpha \cos\delta \ = \ -2.3 \pm 1.6 \text{ mas yr}^{-1} \text{ and} \quad (13)$$

$$\mu_\delta \ = \ 0.2 \pm 1.5 \text{ mas yr}^{-1} \quad (14)$$

and for the field

$$\mu_\alpha \cos\delta \ = \ -0.4 \pm 5.5 \text{ mas yr}^{-1} \text{ and} \quad (15)$$

$$\mu_\delta \ = \ 0.1 \pm 5.5 \text{ mas yr}^{-1}. \quad (16)$$

The measured standard deviation of the cluster proper motion distribution again is the same as was determined for one individual object.

Table 9 shows a list of all proper motions computed.

4.2. Colour magnitude diagram properties

According to the field star subtracted CMD, presented as Fig. 14, NGC 2194 shows a prominent main sequence with a turn-off point near $V = 14.5$ mag and a sparsely populated red giant branch. For this cluster, the proper motion study is not of great value for the isochrone fitting process: As the main sequence turn-off is located around $V = 14.5$ mag, it is clear that the bright blue stars either do not belong to the cluster or do not help in finding the best isochrone fit because of their non-standard evolution like blue stragglers (see, e.g., Stryker 1993). We assume that the presence of the blue bright stars is mainly caused by the coincidence of the field and cluster proper motion centres which causes a certain number of fields stars to be mis-identified as cluster members. As expected in Sect. 4.1, this effect is more dramatic here than in the case of NGC 1960. From the comparison of the isochrones we derived the parameters for NGC 2194 given in Table 8.

Star No. 38 of our sample was first mentioned by del Rio (1980, star 160 therein) who considers this object a field star as a consequence of its location in the CMD. For the same reason, but with the opposite conclusion, Ahumada & Lapasset (1995) mention this object as a cluster member in their "Catalogue of blue stragglers in open star clusters". We find for this star a proper motion of $\mu_\alpha \cos\delta = 2.5$ mas yr^{-1} and $\mu_\delta = -0.1$ mas yr^{-1} leading to a membership probability of 0.34. Therefore, we agree with del Rio and assume star 38 to be a field star, too. So far, no further information is known about the bright blue stars in Fig. 14, so that we cannot give any definite statement about the nature of these objects.

4.3. Initial mass function

The age of NGC 2194 of 550 Myr — together with its distance of almost 3 kpc — implies that the range of the observable main sequence is very limited. We therefore could compute the IMF only over the mass interval from $m \approx 1 M_\odot$ (corresponding to $V \approx 19$ mag) to $m \approx 2.1 M_\odot$ (or $V \approx 15.0$ mag). The slope determined is $\Gamma = -1.33 \pm 0.29$. The comparably higher error is a consequence of the smaller mass interval.

Comparing the resulting IMF with a histogram (see Fig. 16), one finds good agreement for three of the four bins (The bin width is the same as for NGC 1960). As the completeness drops rapidly within the leftmost bin, it has — in total — a high uncertainty. However, only stars with masses of $m > 1 M_\odot$ (corresponding to a completeness of higher than 60%) were taken into consideration for the IMF computation, which is indicated by the limits of the IMF line in Fig. 16.

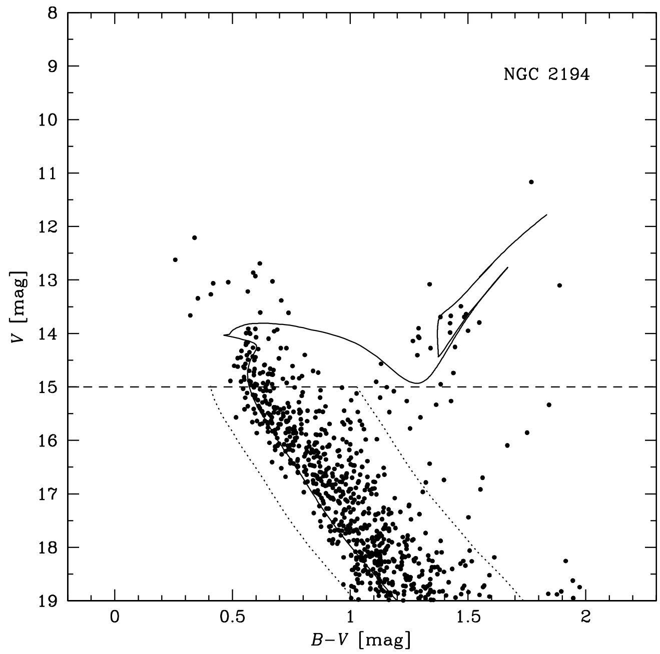

Fig. 14. Colour magnitude diagram of all members of NGC 2194 as determined with the proper motions ($V < 15$ mag) and the statistical field star subtraction ($V > 15$ mag). For more information see Fig. 10

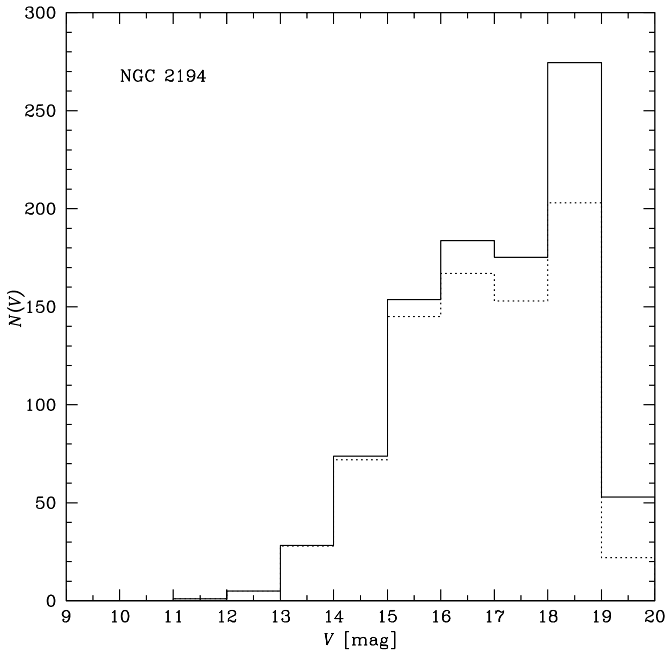

Fig. 15. Luminosity function of NGC 2194. As before, the solid line stands for the completeness corrected data, the dotted line for the uncorrected values. Again, the rightmost bin touches the limiting magnitude of our photometry

Note that as a consequence of the age of NGC 2194, the cluster may have encountered dynamical evolution during its lifetime, which has to be kept in mind when using the term "*initial* mass function". However, we follow Scalo's (1986) nomenclature, who uses the expression for intermediate age clusters, to discriminate between a mass function based on the initial and the present day stellar masses.

5. Summary and discussion

With our work we found NGC 1960 to be a young open star cluster with an age of 16 Myr. It is located at a distance of 1300 pc from the Sun. These results confirm the findings of Barkhatova et al. (1985) obtained with photographic photometry.

We derived proper motions of 404 stars in the region of the cluster down to 14 mag. 178 of those can be considered members of NGC 1960. Despite the problems with our proper motion determination (see Sect. 3.1), we are able to state that our results do not support the values given as the absolute proper motion of NGC 1960 by Glushkova et al. (1997) on the base of the "Four Million Star Catalog" (Gulyaev & Nesterov 1992): They found $\mu_\delta = -8.2 \pm 1$ mas yr^{-1} which is in agreement with our study, but $\mu_\alpha \cos\delta = 14.7 \pm 1$ mas yr^{-1} which differs from our result by more than 10 mas yr^{-1}.

Our study of the IMF of NGC 1960 led to a power law with a slope of $\Gamma = -1.23 \pm 0.17$. This value is very high (i.e. the IMF is shallow) compared to other studies, however, it still matches the interval for Γ suggested by Scalo (1998) for intermediate mass stars ($-2.2 \le \Gamma \le -1.2$).

Although we should stress that we cannot say anything about the shape of the IMF in the very low mass range ($m \ll M_\odot$), we do not see any evidence for a flattening of the IMF of NGC 1960 below $1 M_\odot$.

NGC 2194 — with an age of 550 Myr — belongs to the intermediate age galactic open star clusters. Our findings from the photometric study are in good agreement with the photographic RGU photometry published by del Rio (1980).

As the cluster is located at a distance of almost 3 kpc we could only cover its mass spectrum down to $1 M_\odot$. Nevertheless, we were able to determine the IMF on the base of 623 main sequence stars which led to a slope of $\Gamma = -1.33 \pm 0.29$, almost Salpeter's (1955) value, but still close to the shallow end of the interval given by Scalo (1998).

In our previous paper (Sanner et al. 1999), we studied the open star cluster NGC 581 (M 103) for which we found the same age of 16 ± 4 Myr as for NGC 1960, but a much steeper IMF slope of $\Gamma = -1.80 \pm 0.19$. We therefore can state that our method of IMF determination does not systematically lead to steep or shallow mass functions.

With our yet very small sample, it is not possible to find evidence for the dependence of the IMF of open star clusters on any parameter of the cluster. Therefore, we will have to investigate further clusters and also compare our results with other studies.

Acknowledgements. The authors thank Wilhelm Seggewiss for allocating observing time at the telescopes of Hoher List Observatory, Santi Cassisi for providing the isochrones necessary for our study and Andrea Dieball and Klaas S. de Boer for carefully reading the

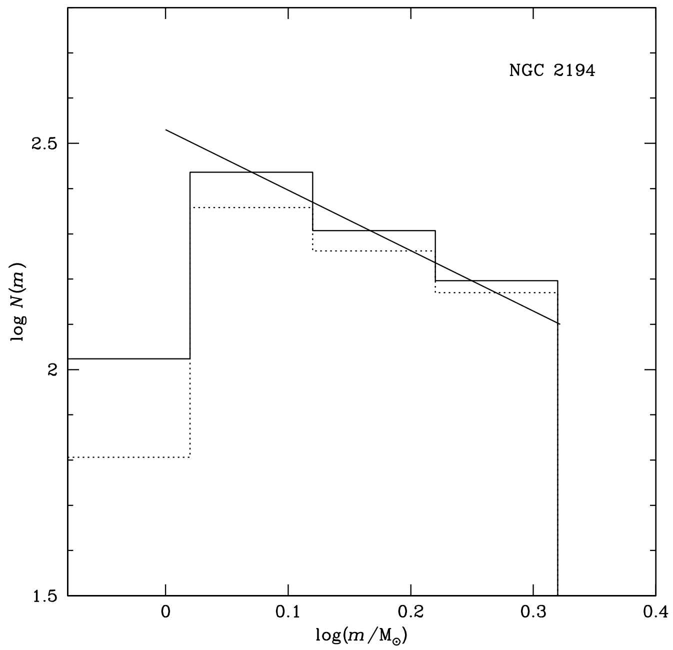

Fig. 16. Initial mass function of NGC 2194. The solid histogram corresponds to the completeness corrected values, the dotted one to the original data. The IMF slope is determined to be $\Gamma = -1.33 \pm 0.29$. Note that the slope was determined with a maximum likelihood analysis; the histogram is only plotted for demonstration. The length of the line illustrates the mass interval for which the IMF was computed

manuscript. J.S. thanks Georg Drenkhahn for his valuable hints concerning the maximum likelihood analysis software. M.A. and J.B. acknowledge financial support from the Deutsche Forschungsgemeinschaft under grants Bo 779/21 and ME 1350/3-2, respectively. This research has made use of NASA's Astrophysics Data System Bibliographic Services, the CDS data archive in Strasbourg, France, and J.-C. Mermilliod's WEBDA database of open star clusters.

References

Abt H.A., 1979, AJ 84, 1591
Ahumada J., Lapasset E., 1995, A&AS 109, 375
Barkhatova K.A., Zakharova P.E., Shashkina L.P., Orekhova L.K., 1985, AZh 62, 854
Bertelli G., Bressan A., Chiosi C., Fagotto F., Nasi E., 1994, A&AS 106, 275
Boden E., 1951, Uppsala Ann. 3, 1
Bono G., Caputo F., Cassisi S., Castellani V, Marconi M., 1997, ApJ 479, 279
Brunzendorf J., Meusinger H., 1998, Astrometric properties of the Tautenburg Plate Scanner. In: Brosche P., Dick W.R., Schwarz O. et al. (eds.) The Message of the Angles — Astrometry from 1798 to 1998. Verlag Harri Deutsch, Thun, Frankfurt a.M., p. 148
Brunzendorf J., Meusinger H., 1999, A&AS 139,141
Chian B., Zhu G., 1966, Ann. Shesan Sect. of Shanghai Obs. 26, 63
del Rio G., 1980, A&AS 42, 189
Dieball A., Grebel E.K., 1998, A&A 339, 773
ESA, 1997, The HIPPARCOS and Tycho Catalogues, ESA SP–1200
Geffert M., Klemola A.R., Hiesgen M., Schmoll J., 1997, A&AS 124, 157
Glushkova E.V., Zabolotskikh M.V., Rastorguev A.S., Uglova I.M., Fedorova A.A., 1997, PAZh 23, 90
Gulyaev A.P., Nesterov V.V., 1992, On the four-million star catalog, Izd. Mos. Gos. Univ.
Iben I., 1965, ApJ 141, 993
Johnson H.L., Morgan W.W., 1953, ApJ 117, 313
Landolt A.U., 1992, AJ 104, 340
Lyngå G., 1987, Catalog of open cluster data, 5$^{\text{th}}$ edition
Meurers J., 1958 , Z. Astrophys. 44, 203
Mermilliod J.-C., 1999, WEBDA: Access to the Open Cluster Database. In: R. Rebolo (ed.) Very Low-Mass Stars and Brown Dwarfs. Cambridge Univ. Press, Cambridge (in press)
Raboud D., Mermilliod J.-C., 1998, A&A 333, 897
Reif K., de Boer K.S., Mebold U. et al., 1995, AG Abstr. Ser. 11, 42
Röser S., Morrison J., Bucciarelli B., Lasker B., McLean B., 1998, Contents, Test Results, and Data Availability for GSC 1.2. In: McLean B., Golombek D.A., Hayes J.J.E., Payne H.E. (eds.) Proc. IAU Symp. 179, New Horizons from Multi-Wavelength Sky Surveys. Kluver, Dordrecht, p. 420
Sagar R., Richtler T., 1991, A&A 250, 324
Salpeter E.E., 1955, ApJ 121, 161
Sanders W.L., 1971, A&A 14, 226
Sanner J., Dieball A., Schmoll J., Reif K., Geffert M., 1998, HoLiCam — A new device for astrometry. In: López García A., Yagudin L., Martínez Usó M. et al. (eds.) IV International Workshop on Positional Astronomy and Celestial Mechanics. Observatorio Astronómico de la Universitat de Valéncia, Valéncia, p. 373
Sanner J., Geffert M., Brunzendorf J., Schmoll J., 1999, A&A 349, 448
Scalo J.M., 1986, Fund. Cosm. Phys. 11, 1
Scalo J.M., 1998, The IMF revisited — A case for variations. In: Gilmore G., Howell D. (eds.) ASP Conf. Series 142. ASP, San Francisco, p. 201
Schaller G., Schaerer D., Meynet G., Maeder A., 1992, A&AS 96, 269
Slettebak A., 1985, ApJS 59, 769
Stetson P.B., 1991, Initial experiments with DAOPHOT II and WFC images. In: Grosbøl P.J., Warmels R.H. (eds.) 3$^{\text{rd}}$ ESO/ST-ECF Garching Data Analysis Workshop. ESO, Garching , p. 187
Stryker L.L., 1993, PASP 105, 1081
Tarrab I., 1982, A&A 109, 285
Tsujimoto T., Yoshii Y., Nomoto K. et al., 1997, ApJ 483, 228
Tucholke H.-J., 1992, A&AS 93, 293
Urban S.E., Corbin T.E., Wycoff G.L., 1998, AJ 115, 2161
van Leeuwen F., 1985, Proper Motion Studies of Stars in and Around Open Clusters. In: Goodman J., Hut P. (eds.) Proc. IAU Symp. 113, Dynamics of star clusters. Reidel, Dordrecht, p. 579
Wielen R., Dettbarn C., Jahreiß H., Lenhardt H., Schwan, H., 1999, A&A 346, 675
Zorec J., Briot D., 1991, A&A 245, 150